Science Advances

AAAS

advances.sciencemag.org/cgi/content/full/4/1/eaao5348/DC1

Supplementary Materials for

Detecting reciprocity at global scale

Morgan R. Frank, Nick Obradovich, Lijun Sun, Wei Lee Woon, Brad L. LeVeck, Iyad Rahwan

Published 3 January 2018, *Sci. Adv.* **4**, eaao5348 (2018)
DOI: 10.1126/sciadv.aao5348

This PDF file includes:

- fig. S15. The effects of biased news data ($\lambda = 0.40$).
- fig. S16. The effects of biased news data ($\lambda = 0.50$).
- fig. S17. The effects of biased news data ($\lambda = 0.60$).
- fig. S18. The effects of biased news data ($\lambda = 0.70$).
- fig. S19. The effects of biased news data ($\lambda = 0.80$).
- fig. S20. The effects of biased news data ($\lambda = 0.90$).
- fig. S21. Main results using CCM analysis with $E = 200$ and $\tau = 2$.
- fig. S22. Main results using CCM analysis with $E = 200$ and $\tau = 3$.
- fig. S23. Main results using CCM analysis with $E = 200$ and $\tau = 4$.
- fig. S24. Main results using CCM analysis with $E = 200$ and $\tau = 5$.
- fig. S25. Country pairs exhibiting CCM reciprocity are more likely to reciprocate cooperation or conflict.
- fig. S26. The patterns of behavior in the day following an interaction.
- fig. S27. The patterns of behavior in the three days following an interaction.
- fig. S28. The patterns of behavior in the week following an interaction.
- fig. S29. The patterns of behavior in the month following an interaction.
- fig. S30. The effects of varying the CCM threshold for causality.
- fig. S31. Pairs of countries exhibiting CCM reciprocity [that is, $\text{CCM}(A, B) \geq 0.15$ and $\text{CCM}(B, A) \geq 0.15$] are connected using yellow edges.
- fig. S32. Pairs of countries exhibiting CCM reciprocity [that is, $\text{CCM}(A, B) \geq 0.15$ and $\text{CCM}(B, A) \geq 0.20$] are connected using yellow edges.
- fig. S33. Pairs of countries exhibiting CCM reciprocity [that is, $\text{CCM}(A, B) \geq 0.15$ and $\text{CCM}(B, A) \geq 0.25$] are connected using yellow edges.
- fig. S34. Pairs of countries exhibiting CCM reciprocity [that is, $\text{CCM}(A, B) \geq 0.15$ and $\text{CCM}(B, A) \geq 0.30$] are connected using yellow edges.
- fig. S35. Pairs of countries exhibiting CCM reciprocity [that is, $\text{CCM}(A, B) \geq 0.15$ and $\text{CCM}(B, A) \geq 0.35$] are connected using yellow edges.
- fig. S36. Pairs of countries exhibiting CCM reciprocity [that is, $\text{CCM}(A, B) \geq 0.15$ and $\text{CCM}(B, A) \geq 0.40$] are connected using yellow edges.
- fig. S37. Pairs of countries exhibiting CCM reciprocity [that is, $\text{CCM}(A, B) \geq 0.15$ and $\text{CCM}(B, A) \geq 0.45$] are connected using yellow edges.
- fig. S38. Pairs of countries exhibiting CCM reciprocity [that is, $\text{CCM}(A, B) \geq 0.15$ and $\text{CCM}(B, A) \geq 0.50$] are connected using yellow edges.
- table S1. Nations ordered by total imposed influence.
- table S2. The Pearson correlation for proportion of interactions of each quad class between a pair of countries to the shared influence for that pair of countries.
- table S3. Country pairs ordered by increasing absolute difference in directed influence [that is, $\text{CCM}(A, B) - \text{CCM}(B, A)$].

section S1. Summarizing ICEWS

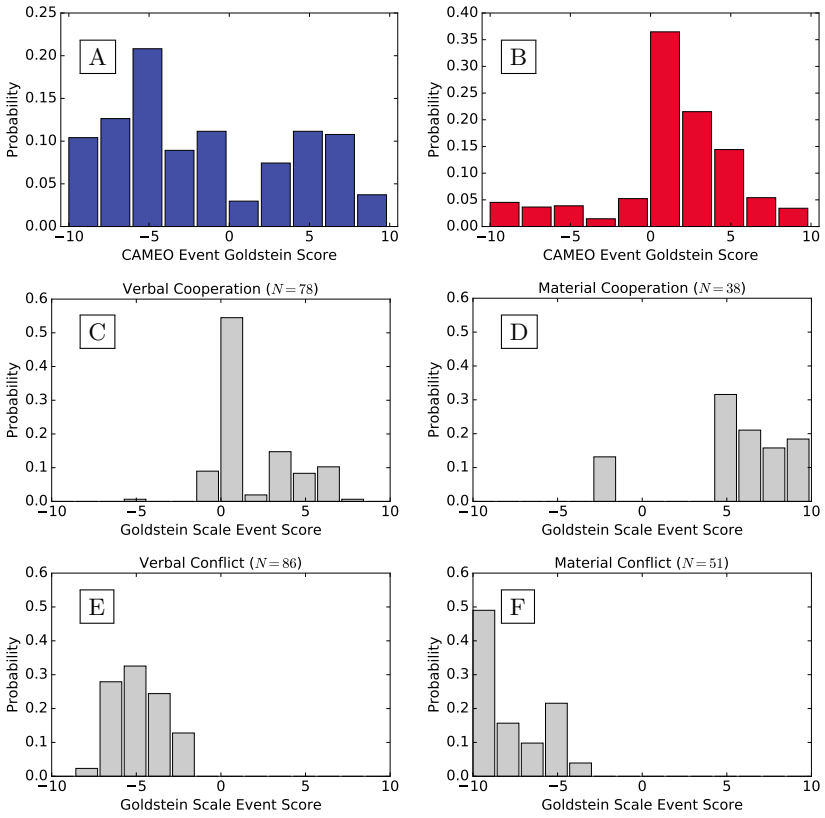

fig. S1. The distributions of Goldstein scores by CAMEO event type occurring in the ICEWS data set.

The distributions of Goldstein scores by CAMEO event type occurring in the ICEWS dataset **(A)** and weighted by the frequency of occurrence in ICEWS **(B)**. For both panels, event types are binned according to $g_e \in \{[-10, -8), [-8, -6), \ldots, [6, 8), [8, 10]\}$. The distribution of Goldstein scores by CAMEO event type according to Quad Class: Verbal Cooperation **(C)**, Material Cooperation **(D)**, Verbal Conflict **(E)**, and Material Conflict **(F)**.

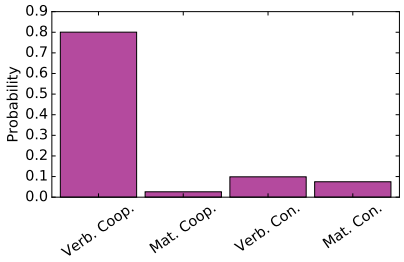

fig. S2. The distribution of CAMEO Quad Classes in the ICEWS data set.

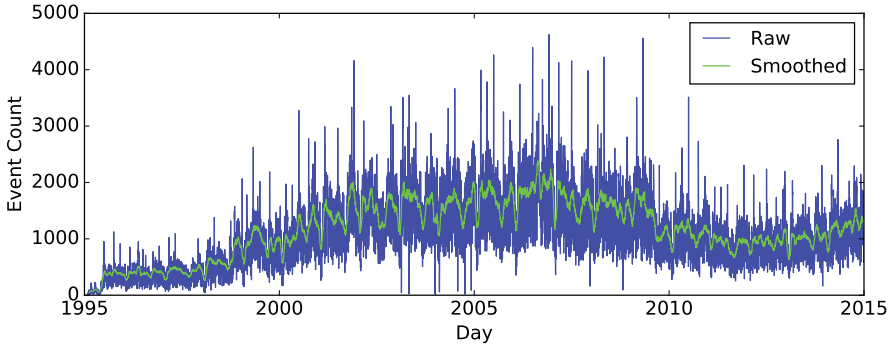

fig. S3. The number of events per day during the entire ICEWS data set. The green line represents a 30-day moving average.

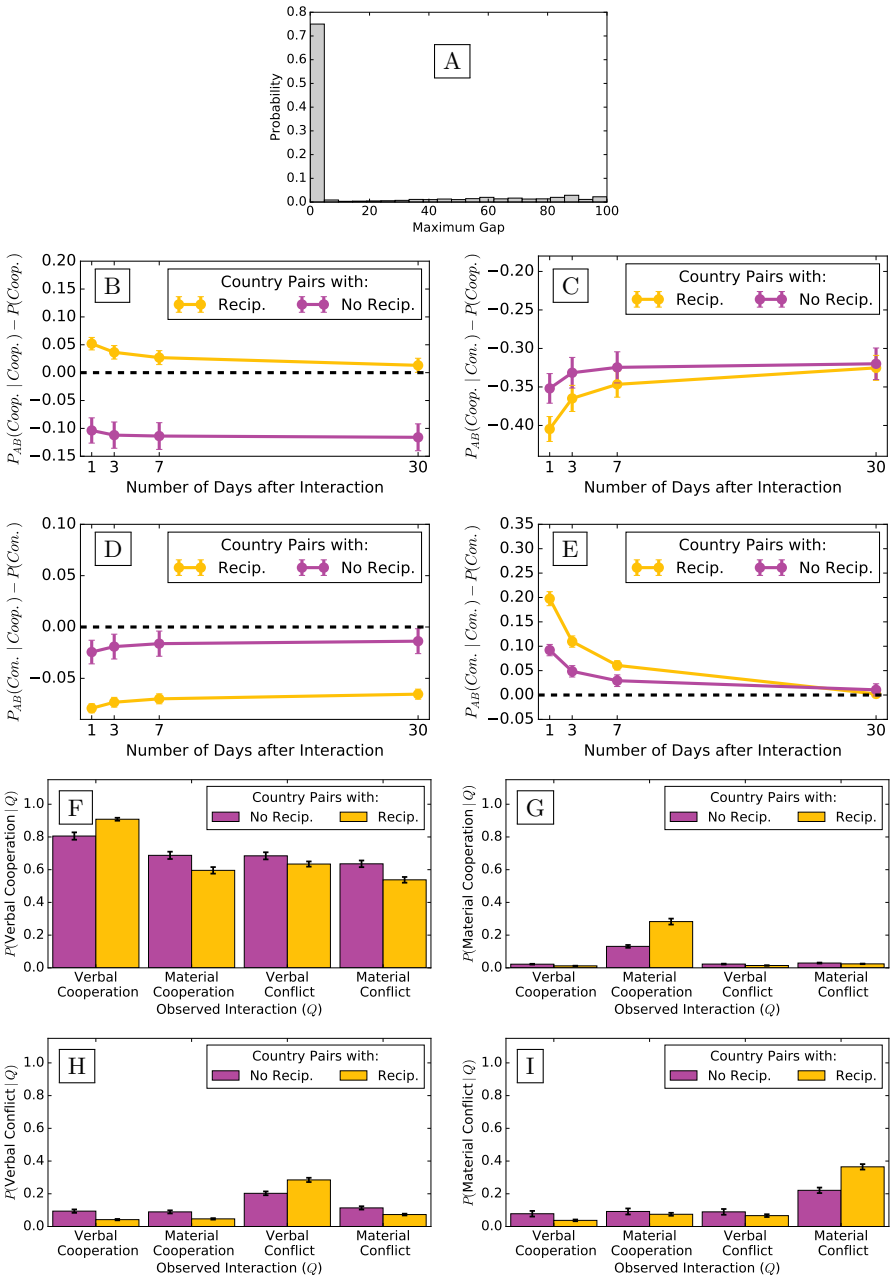

fig. S4. Gaps in interactions between country pairs are small. **(A)** The distribution of maximum time periods without interaction data for country pairs considered for CCM analysis. For plots (B)-(I), we use cubic spline interpolation instead of linear interpolation for missing data. **(B)-(E)** Analogous plots to Figure 2 in the main text. **(F)-(I)** Analogous plots to Figure 3 in the main text. The main results remain unchanged.

section S2. Measuring influence using CCM

Convergent Cross Mapping (CCM) is a recently proposed method for detecting causality between variables in both dynamical systems and empirical studies (33,43). The idea is that if variable X "causes" variable Y, then information about the trajectory of X is recoverable from Y. With CCM, we are treating the system as a dynamical system (i.e. X and Y are dynamically related) rather than purely stochastic relationships, and testing if time-lagged neighborhoods of X correspond to time-lagged neighborhoods of Y.

Specifically, we must first consider the system of interest as a dynamical system with some kind of long-time attractor behavior. If the system diverges to infinity or converges to a set of fixed points, then the system is very predictable in the long-run and therefore does not require CCM to understand long-time system dynamics. It remains to consider systems with periodic (but noisy) or strange attractors; such systems are typically inherent in the complex systems we are interested in, such as the system of international relations.

Let's consider the classic Lorenz attractor as an example dynamical system exhibiting chaotic temporal dynamics. This system is governed by the set of equations

$$dX/dt = \sigma(Y - X) \tag{1}$$
$$dY/dt = X(\rho - Z) - Y \text{ and} \tag{2}$$
$$dZ/dt = XY - \beta Z \tag{3}$$

Let $\sigma = 10$, $\rho = 28$, and $\beta = 8/3$. We begin with a random initial state within the unit box and integrate 10^6 iterations with a time step of $dt = 0.01$ using the Runge-Kutta method of order 4 to remove transient dynamics. We then integrate another 10^5 iterations to produce a trajectory which approximates the strange attractor of the Lorenz equation (see Fig. 5 for an example trajectory).

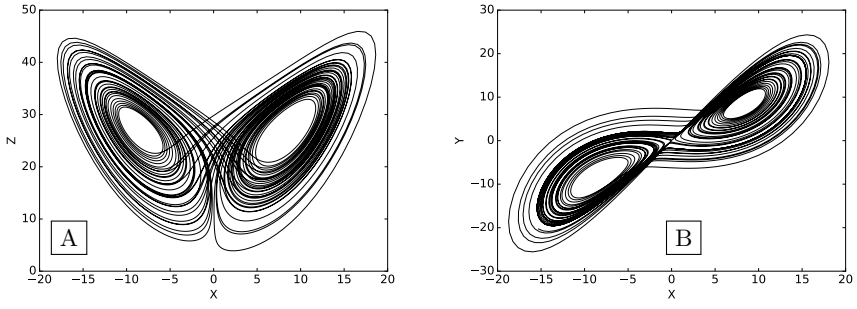

fig. S5. An example from dynamical systems.
The classic Lorenz '63 attractor with $\sigma = 10$, $\rho = 28$, and $\beta = 8/3$ as seen in the **(A)** X-Z plane and the **(B)** X-Y plane.

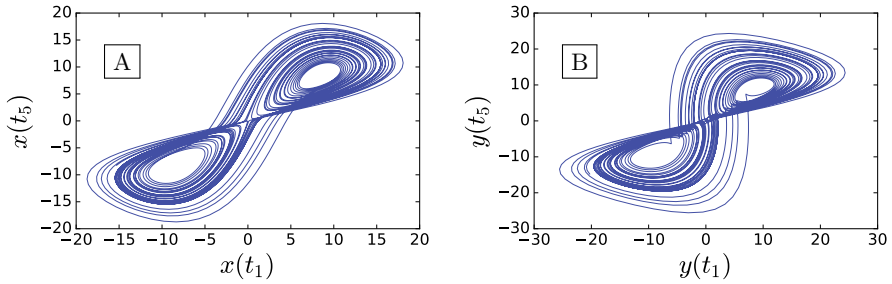

fig. S6. Examples of shadow manifolds. The shadow manifolds **(A)** M_X and **(B)** M_Y.

Consider the time series of variables X and Y for the system attractor. Since we have assumed the system is bounded and not fixed, the trajectories X and Y must each come near to themselves occasionally. CCM measures if the nearby points on X correspond to nearby points on Y; if so, then X can be used to reconstruct Y and we say that Y "CCM causes" X. We know that longer trajectories for dynamical systems with strange attractors produce better approximations of the attractor, and, likewise, provides better potential for CCM to reproduce variables skillfully because the improvements in attractor approximation leads to closer sets of nearby points in X and Y.

Consider a trajectory about some attractor of length L (i.e. a trajectory of L equidistant time steps), and let $X(t)$ and $Y(t)$ be the trajectories of the variables X and Y in this system. We form temporally-lagged approximations of X according to $x(t) = \{X(t), X(t-\tau), X(t-2\tau), \ldots, X(t-(E-1)\tau)\}$ for $t = 1+(E-1)\tau$ to $t = L$ which we call the "reconstructed manifold" or "shadow manifold" M_X. Here, τ represents a time-lag variable and E determines the dimensional embedding of the manifold. Note that higher dimensional embeddings (i.e. larger E) lead to greater potential to capture system dynamics in a shadow manifold, but only to a point after which the computational complexity of the CCM algorithm increases without increasing its effectiveness. In other words, we expect that CCM's ability to reconstruct Y from X will converge as L increases. Figure 6 exhibits example shadow manifolds for the Lorenz attractor.

Now we identify the $E+1$ nearest neighbors of $x(t)$ from nearest to furthest according to the indices $t_1, t_2, \ldots, t_{E+1}$. Let $d(x(t), x(t_i))$ denote the euclidean distance between $x(t)$ and $x(t_i)$, and let

$$u_i = \exp\big(-d(x(t), x(t_i))/d(x(t), x(t_1))\big) \tag{4}$$

denote a rescaling of the distances amongst nearest neighbors to $x(t)$ (recall $x(t_1)$ represents the nearest neighbor to $x(t)$). We use these rescaled distances to produce weights for each nearest neighbor index according to

$$w_i = u_i / \sum_{j=1}^{E+1} u_j \tag{5}$$

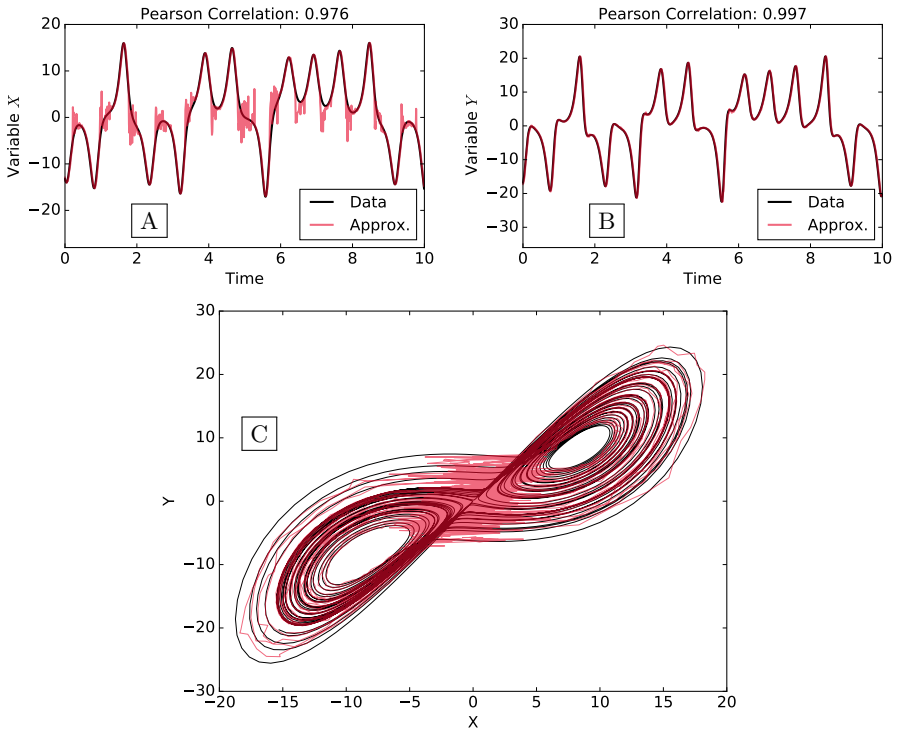

fig. S7. Using nearest neighbors of shadow manifolds to recover variable dynamics. **(A)** $\hat{X}(t)|M_Y$ (in red) compared to $X(t)$ (in black). **(B)** $\hat{Y}(t)|M_X$ (in red) compared to $Y(t)$ (in black). **(C)** We plot the true X-Y trajectory in black and compare to the trajectory defined by $\hat{X}(t)|M_Y$ and $\hat{Y}(t)|M_X$ in red. The approximation is very good except around the origin, where prediction is known to be hardest for the Lorenz system.

and, finally, we reconstruct $Y(t)$ given M_x according to

$$Y(t)|M_X = \sum_{i=1}^{E+1} w_i \cdot Y(t_i) \tag{6}$$

We repeat the calculation for each time in the trajectories of X and Y to produce a trajectory that hopefully approximates the true trajectory $Y(t)$. We provide examples of reconstructed trajectories in Figure 7 using the Lorenz attractor. There are many methods to measure the similarity between pairs of time series, but we focus on the Pearson correlation between the empirical and reconstructed time series to assess CCM's ability to reconstruct the temporal dynamics of one variable given the other. That is, in the most ideal sense, a Pearson correlation coefficient of $\rho = 1$ indicates that the reconstructed time series completely predicts the true time series. We use $CCM(A, B) = \rho$ to denote

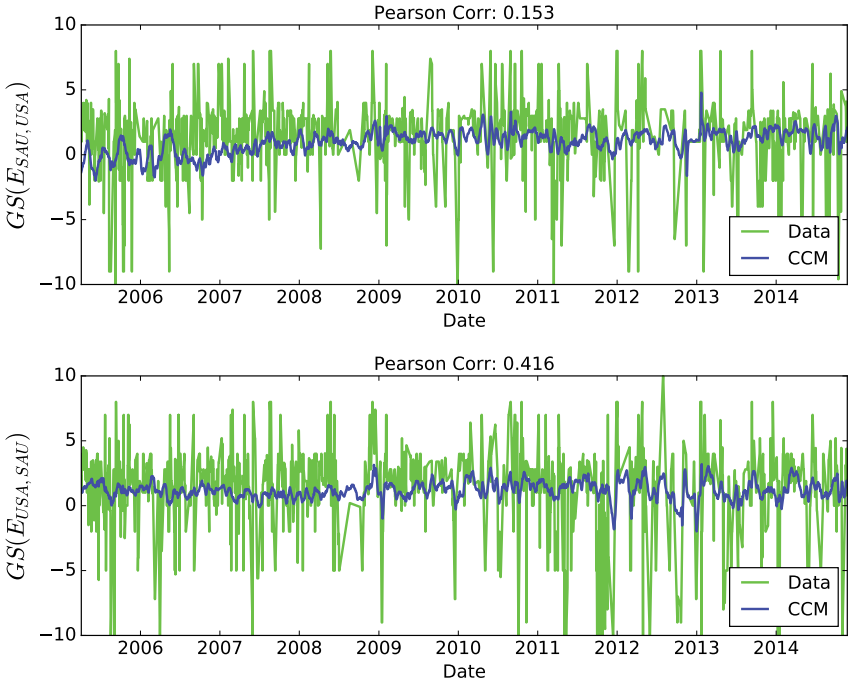

fig. S8. Using CCM to infer causality between using United States (USA) treatment of Saudi Arabia (SAU) and Saudi Arabia's treatment of the United States ($E = 200, \tau = 1$). **(Top)** SAU's treatment of USA does not cause USA's treatment of SAU using the directed daily average Goldstein time series. **(Bottom)** USA's treatment of SAU does cause SAU's treatment of USA using the directed daily average Goldstein time series.

the strength of causality detected from country A to country B. The paper introducing CCM [33] examines some empirical cases and notes that Pearson correlations of around $CCM(A, B) \geq 0.25$ may be sufficient to indicate causation in noisy empirical data. In sections 2.1, 2.2, and 2.3 (below), we provide a stability analysis for CCM as applied to ICEWS data.

For our purposes, CCM can be used to measure causality or influence between time series from the ICEWS data. Figure 8 provides an example case examining the influence between the United States (USA) and Saudi Arabia (SAU) while setting the CCM parameters $E = 200$ and $\tau = 1$ (note: these are the same parameters used for all ICEWS time series comparisons in this study). This selection of E is large enough to capture dynamics in the time series used here, and we demonstrate that our main results are stable to reasonable alternative choices of τ (see Figures 21-24). We apply CCM to infer causality from $E_{USA,SAU}$ and $E_{SAU,USA}$ to determine that USA's treatment of SAU "CCM causes" SAU's treatment of USA ($CCM(USA, SAU) = 0.42$). However, SAU

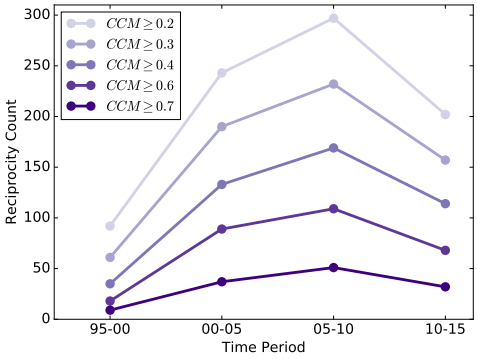

fig. S9. The number of pairs of countries exhibiting CCM reciprocity (y-axis) during four 5-year time periods (x-axis) as we vary the minimum influence threshold (i.e. minimum Pearson correlation of CCM reconstruction, indicated by color).

does not appear to cause USA's treatment of SAU ($CCM(SAU, USA) = 0.15$).

In general, for countries A and B, if $GS(E_{A,B})$ "CCM causes" $GS(E_{B,A})$ and $GS(E_{B,A})$ "CCM causes" $GS(E_{A,B})$, then we will say the countries A and B exhibit "CCM reciprocity". Note that CCM reciprocity does not imply direct reciprocity because, although counter-intuitive, CCM causation between two variables does not imply those variables are correlated. In other words, it may be that country A's cooperative behavior towards country B is causing country B's conflictive behavior towards country A. A deeper examination is undertaken in the main text to further characterize instances of CCM reciprocity amongst pairs of countries, and we uncover evidence that CCM reciprocity is indeed a viable proxy for direct reciprocity.

2.1 Stability analysis for CCM: the effects of random noise

The average Goldstein time series we examine can be very noisy (see Fig. 8 for example), which prompts us to test the effects of random noise on CCM's ability to detect causation. We take the trajectories for variables X and Y from the Lorenz system (also used in Fig. 7) and artificially add uniformly distributed noise to each point on each trajectory according to $\gamma \cdot U(-.5, .5)$ (see Fig. 10A). As we increase γ, we apply the CCM algorithm and note the deterioration of CCM causation between X and Y (see Fig. 9B). The ability for CCM to detect the true causal relationship between variables X and Y deteriorates slowly with increasing γ indicating CCM's robustness to uniform noise which may be inherent in the Goldstein time series we construct from ICEWS data.

2.2 Stability analysis for CCM: the effects of biased sub-sampling

ICEWS is constructed from news sources from around the world, but there is always a risk of biased sampling from countries with larger media presence. Alternatively, news outlets from different countries may be biased through political or economic ties in the coverage of world events. Therefore, we test the robustness of CCM and shared influence (i.e. $(CCM(A,B)+CCM(B,A))/2$) to biased sub-sampling by event type (i.e. Quad Class) while varying the sub-sampling rate.

For each pair of countries, A and B, subject to CCM analysis, for each sub-sampling rate $\lambda \in \{0, 0.1, 0.2, ..., 0.9\}$, and for each Quad Class (i.e. verbal cooperation, material cooperation, verbal conflict, and material conflict), we perform three trials of sub-sampling to test the stability of $CCM(A,B)$ and the stability of shared influence between A and B. Specifically, given the complete set of interactions between countries A and B, and given a Quad Class, Q, we randomly select λ of the total interactions between A and B of Quad Class Q before calculating new directed Goldstein time series and, finally, calculating the resulting influence scores after sub-sampling (i.e. $CCM^*(A,B)$ and $(CCM^*(A,B)+CCM^*(B,A))/2$). We take the difference between the sub-sampled influence scores and the corresponding influence scores using the complete interaction dataset (i.e. $CCM(A,B)$ and $(CCM(A,B)+CCM(B,A))/2$) to assess the impact of biased sub-sampling.

For a given sub-sampling rate, we combine the resulting changes for each pair of countries and each Quad Class into a single distribution of change in influence and a single distribution of change in shared influence for that level of sub-sampling. Figure 11-20 demonstrate the distributions while varying sub-sampling rate (λ). Each distribution reveals a very small median change in influence or shared influence as a result of biased sub-sampling. For example, taking $\lambda = 0.5$ (i.e. Fig. 16) the median change in $CCM(A,B) - CCM^*(A,B)$ is 0.0008 and the median change in shared influence is 0.03. These results suggest that CCM analysis is robust to reasonable amounts of biased sub-sampling by interaction type.

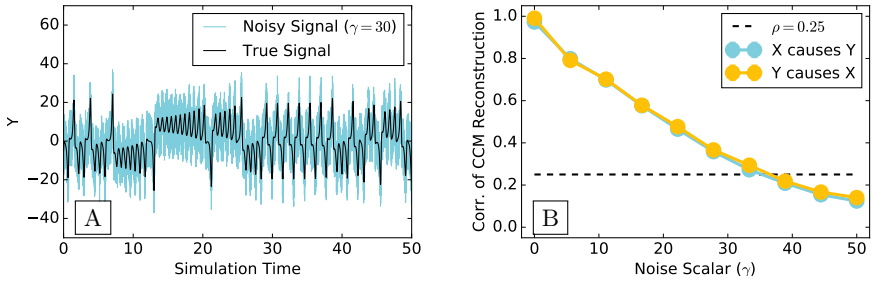

fig. S10. CCM causation decreases with increased artificial noise. **(A)** An example of the true trajectory of the Y variable from the Lorenz system (black) compared to the signal with added uniform noise ($\gamma = 30$, blue). **(B)** Without added noise, the X and Y variables in the Lorenz system are causal of each other, and artificially adding uniform noise to the true trajectories slowly diminishes the CCM causation detected.

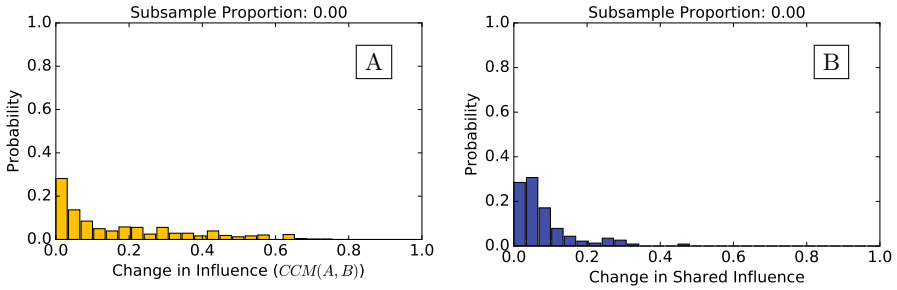

fig. S11. The effects of biased news data ($\boldsymbol{\lambda} = 0.00$). Distributions of change in **(A)** directed influence (i.e. $CCM(A, B)$) and **(B)** shared influence (i.e. $(CCM(A, B) + CCM(B, A))/2$) after biased subsampling by event type (i.e. Quad Class).

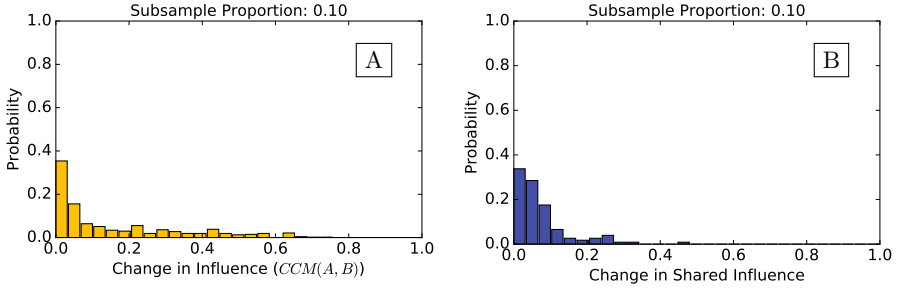

fig. S12. The effects of biased news data ($\boldsymbol{\lambda} = 0.10$). Distributions of change in **(A)** directed influence (i.e. $CCM(A, B)$) and **(B)** shared influence (i.e. $(CCM(A, B) + CCM(B, A))/2$) after biased subsampling by event type (i.e. Quad Class).

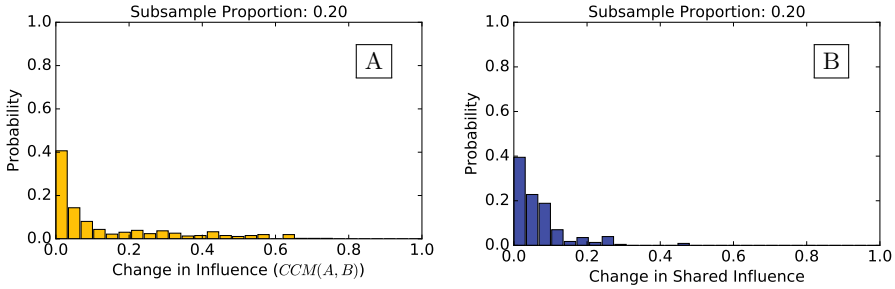

fig. S13. The effects of biased news data ($\lambda = 0.20$). Distributions of change in **(A)** directed influence (i.e. $CCM(A, B)$) and **(B)** shared influence (i.e. $(CCM(A, B)+CCM(B, A))/2$) after biased subsampling by event type (i.e. Quad Class).

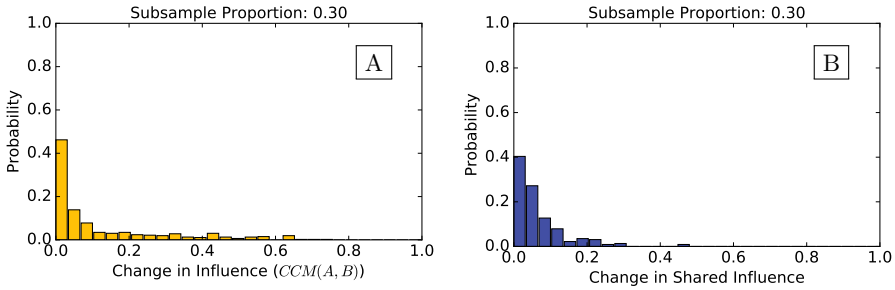

fig. S14. The effects of biased news data ($\lambda = 0.30$). Distributions of change in **(A)** directed influence (i.e. $CCM(A, B)$) and **(B)** shared influence (i.e. $(CCM(A, B)+CCM(B, A))/2$) after biased subsampling by event type (i.e. Quad Class).

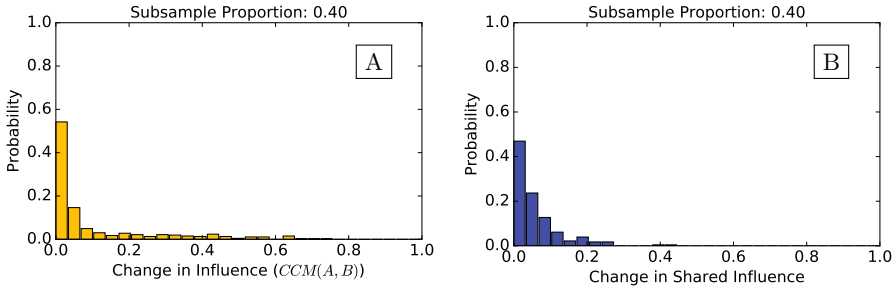

fig. S15. The effects of biased news data ($\lambda = 0.40$). Distributions of change in **(A)** directed influence (i.e. $CCM(A, B)$) and **(B)** shared influence (i.e. $(CCM(A, B)+CCM(B, A))/2$) after biased subsampling by event type (i.e. Quad Class).

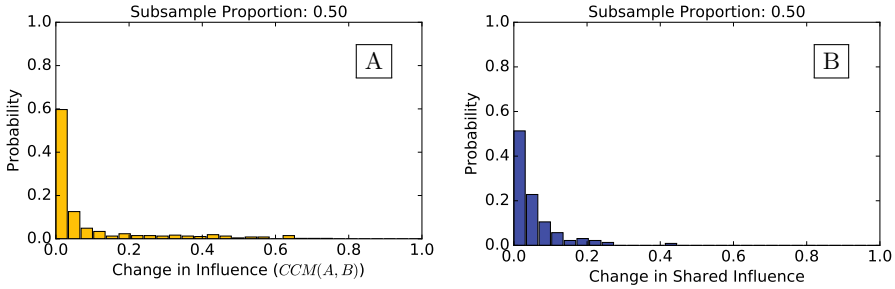

fig. S16. The effects of biased news data ($\lambda = 0.50$).
Distributions of change in **(A)** directed influence (i.e. $CCM(A, B)$) and **(B)** shared influence (i.e. $(CCM(A, B)+CCM(B, A))/2$) after biased subsampling by event type (i.e. Quad Class).

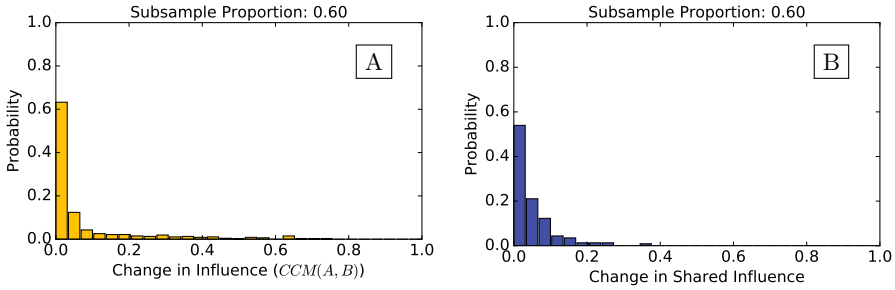

fig. S17. The effects of biased news data ($\lambda = 0.60$).
Distributions of change in **(A)** directed influence (i.e. $CCM(A, B)$) and **(B)** shared influence (i.e. $(CCM(A, B)+CCM(B, A))/2$) after biased subsampling by event type (i.e. Quad Class).

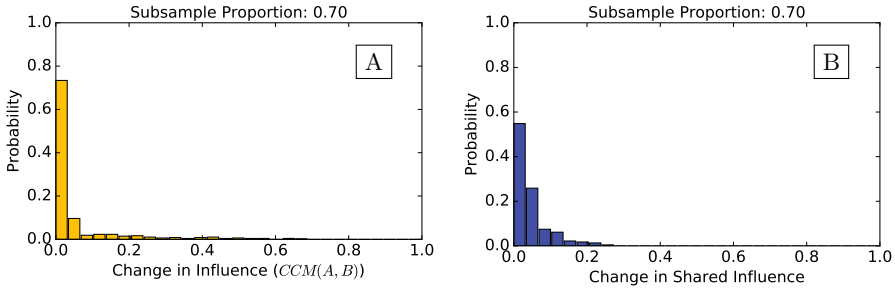

fig. S18. The effects of biased news data ($\lambda = 0.70$).
Distributions of change in **(A)** directed influence (i.e. $CCM(A, B)$) and **(B)** shared influence (i.e. $(CCM(A, B)+CCM(B, A))/2$) after biased subsampling by event type (i.e. Quad Class).

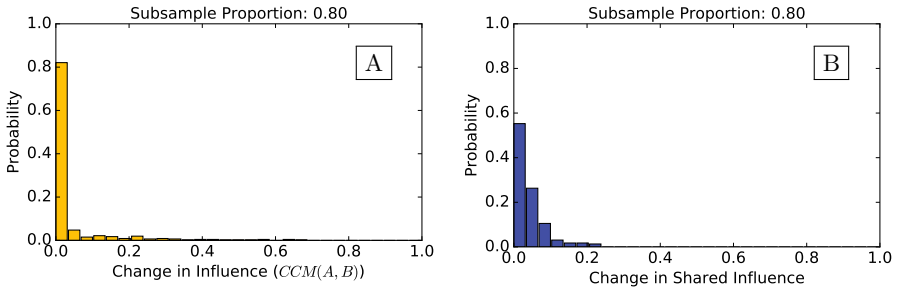

fig. S19. The effects of biased news data ($\lambda = 0.80$).
Distributions of change in **(A)** directed influence (i.e. $CCM(A, B)$) and **(B)** shared influence (i.e. $(CCM(A, B)+CCM(B, A))/2$) after biased subsampling by event type (i.e. Quad Class).

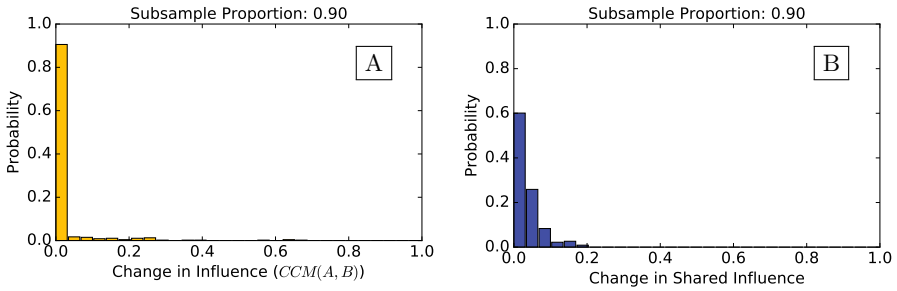

fig. S20. The effects of biased news data ($\lambda = 0.90$).
Distributions of change in **(A)** directed influence (i.e. $CCM(A, B)$) and **(B)** shared influence (i.e. $(CCM(A, B)+CCM(B, A))/2$) after biased subsampling by event type (i.e. Quad Class).

2.3 Stability analysis for CCM: varying τ

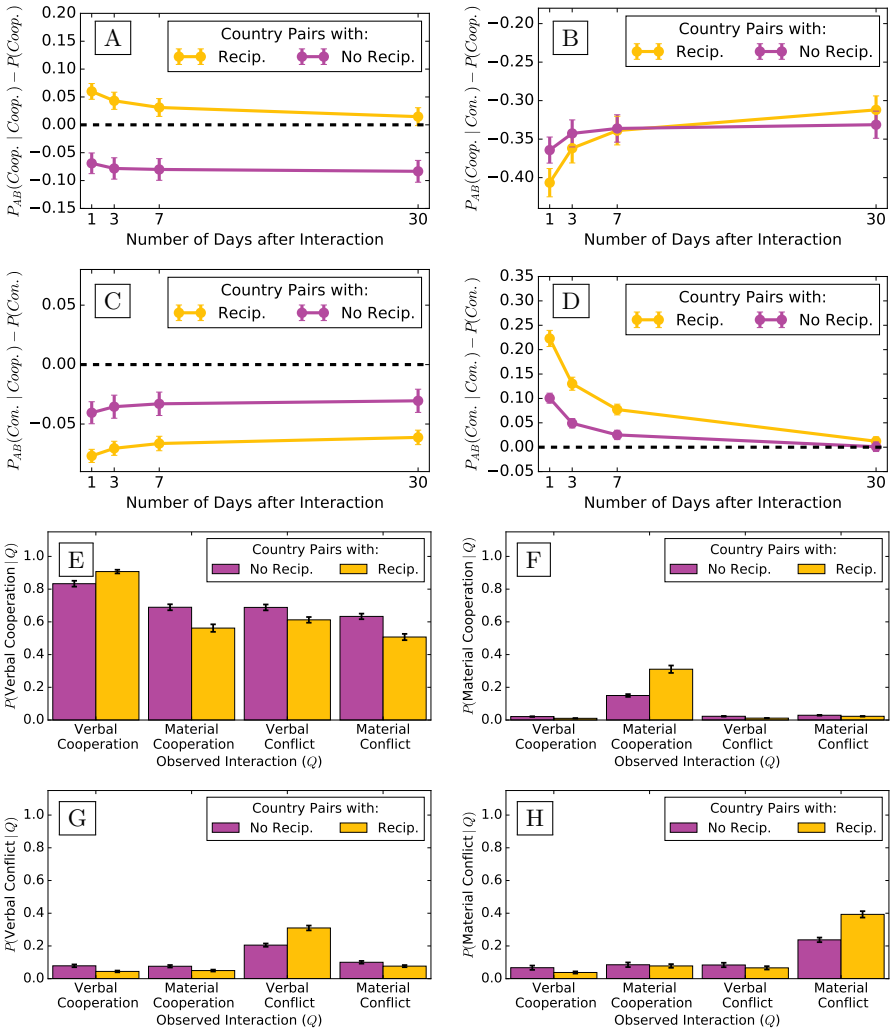

Figure 21: Main results using CCM analysis wih $E = 200$ and $\tau = 2$. **(A)-(D)** Analogous plots to Figure 2 in the main text. **(E)-(H)** Analogous plots to Figure 3 in the main text.

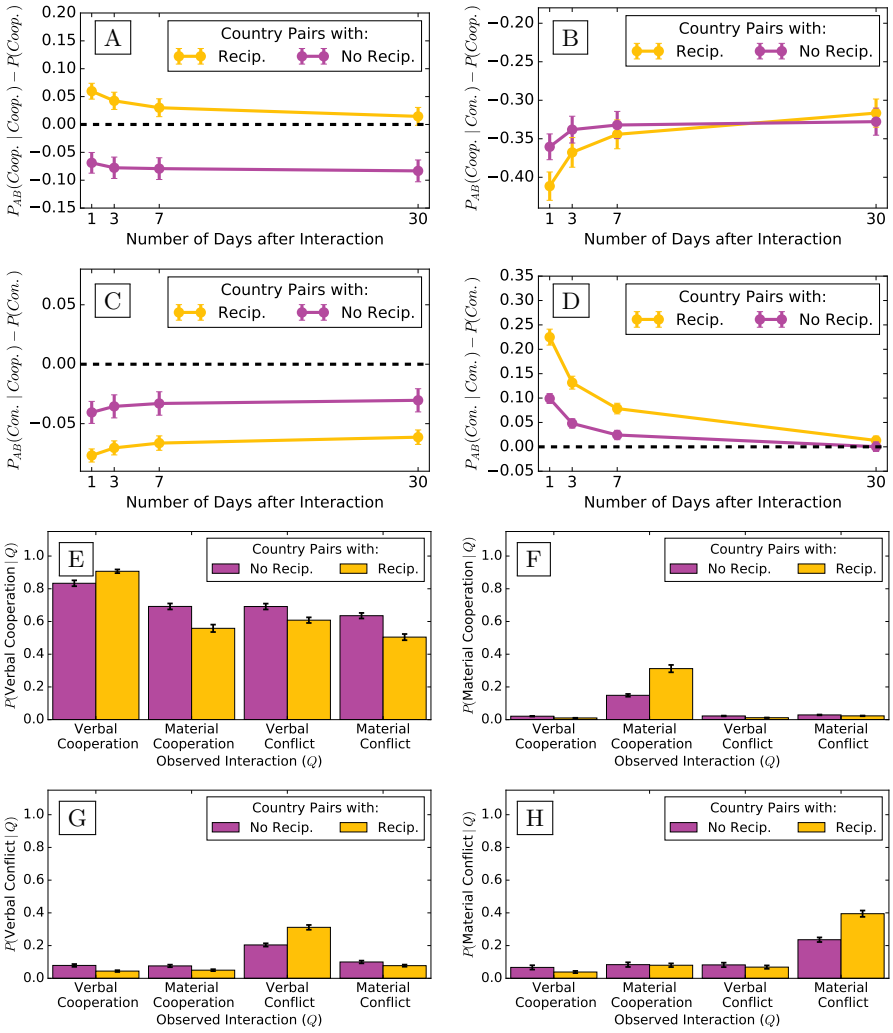

Figure 22: Main results using CCM analysis wih $E = 200$ and $\tau = 3$. **(A)-(D)** Analogous plots to Figure 2 in the main text. **(E)-(H)** Analogous plots to Figure 3 in the main text.

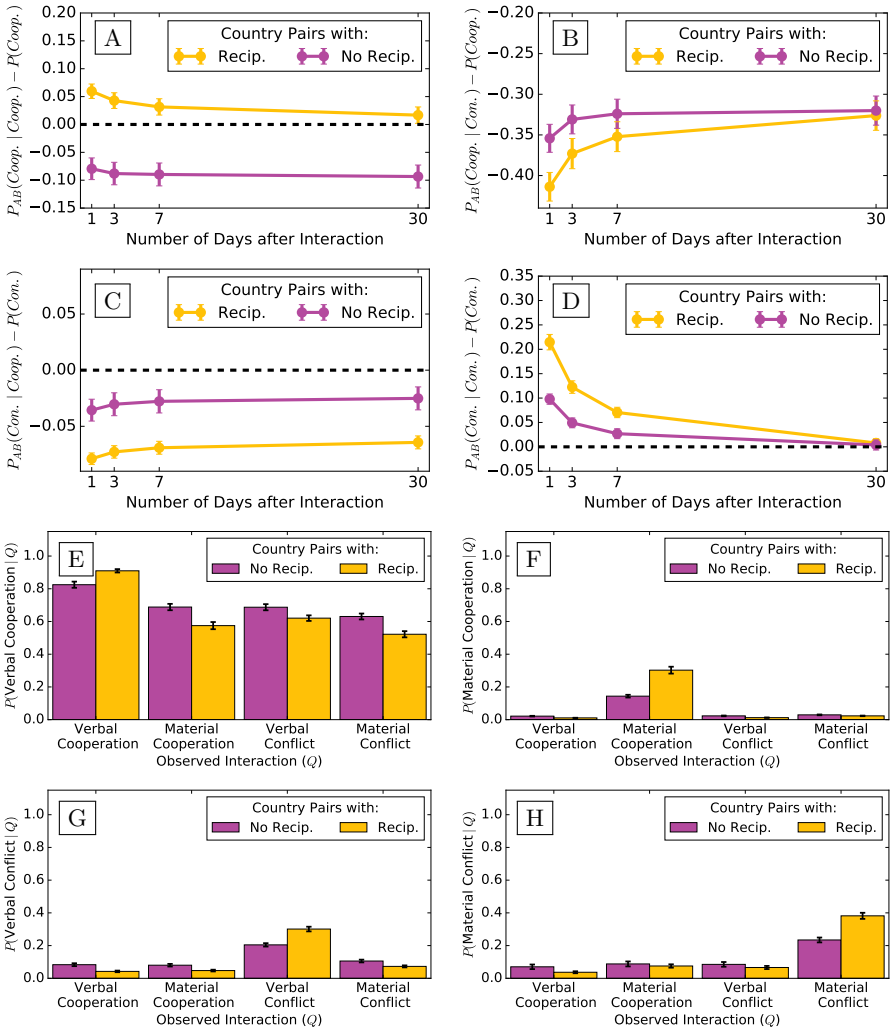

Figure 23: Main results using CCM analysis wih $E = 200$ and $\tau = 4$. **(A)-(D)** Analogous plots to Figure 2 in the main text. **(E)-(H)** Analogous plots to Figure 3 in the main text.

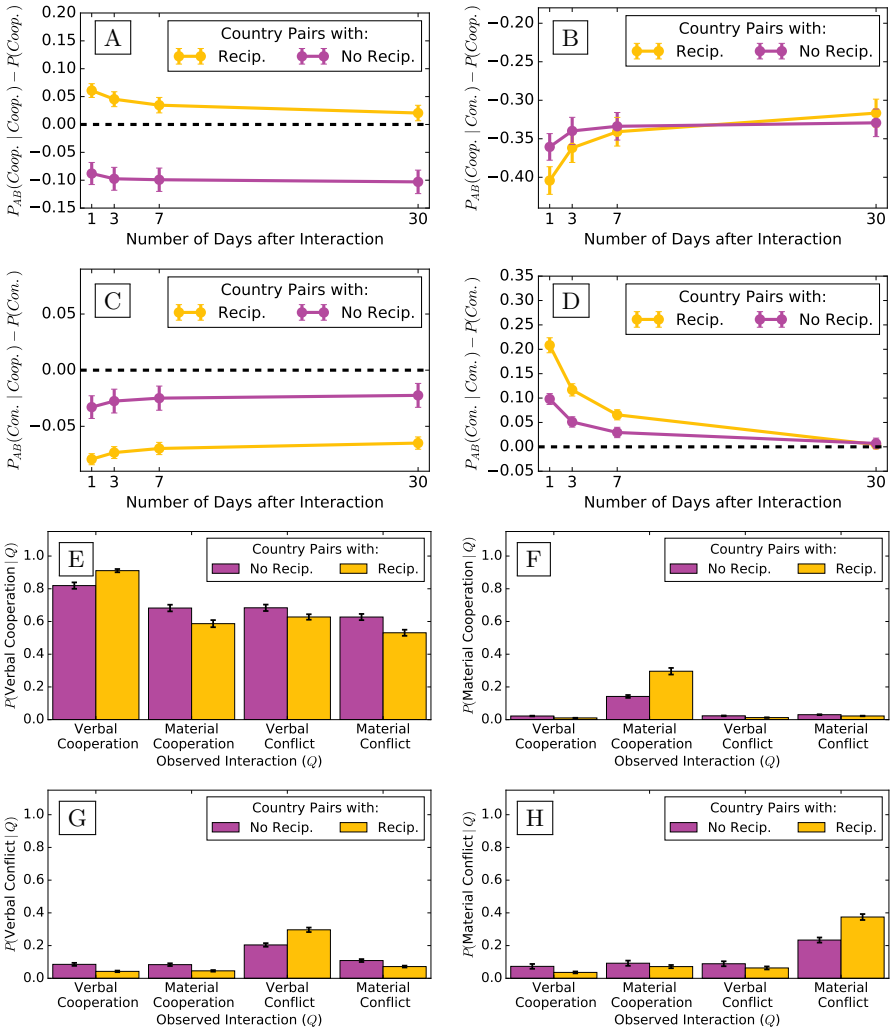

Figure 24: Main results using CCM analysis wih $E = 200$ and $\tau = 5$. **(A)-(D)** Analogous plots to Figure 2 in the main text. **(E)-(H)** Analogous plots to Figure 3 in the main text.

2.4 Nations Ordered by Influence

table S1. Nations Ordered by total imposed influence.

Nation	Number of Influential Relations	Total Imposed Influence	Average Imposed Influence
United States	35	7.330	0.209
United Kingdom	10	3.957	0.396
Russia	13	3.404	0.262
China	12	3.251	0.271
France	9	3.049	0.339
Turkey	6	2.074	0.346
Japan	7	1.980	0.283
Egypt	6	1.975	0.329
Germany	6	1.831	0.305
Italy	4	1.819	0.455
Jordan	4	1.548	0.387
Poland	3	1.499	0.500
Israel	5	1.450	0.290
Croatia	3	1.439	0.480
Iran	7	1.348	0.193
Syria	5	1.332	0.266
Thailand	3	1.030	0.343
Greece	2	1.030	0.515
Cyprus	2	0.978	0.489
Ireland	2	0.946	0.473
Ukraine	3	0.936	0.312
Taiwan	3	0.912	0.304
South Africa	2	0.874	0.437
South Korea	4	0.861	0.215
North Korea	3	0.831	0.277
Spain	2	0.788	0.394
Cambodia	2	0.782	0.391
Bosnia and Herzegovina	2	0.708	0.354
Tanzania	1	0.697	0.697
Latvia	1	0.689	0.689
Serbia	2	0.681	0.341
Pakistan	4	0.668	0.167
Palestine	4	0.641	0.160
Uganda	1	0.637	0.637
Lithuania	1	0.629	0.629
Rwanda	1	0.627	0.627
Iraq	3	0.617	0.206
Kenya	1	0.609	0.609
Canada	1	0.545	0.545
Yemen	1	0.529	0.529

Indonesia	2	0.494	0.247
Vietnam	2	0.489	0.245
Colombia	2	0.487	0.244
Afghanistan	2	0.448	0.224
Australia	3	0.399	0.133
Azerbaijan	1	0.396	0.396
Brazil	1	0.383	0.383
Hong Kong	1	0.377	0.377
Lebanon	2	0.365	0.182
Georgia	2	0.358	0.179
Saudi Arabia	2	0.353	0.176
Venezuela	1	0.312	0.312
Kyrgyzstan	1	0.299	0.299
Belarus	1	0.282	0.282
Argentina	1	0.277	0.277
Myanmar	1	0.262	0.262
India	1	0.258	0.258
Kazakhstan	1	0.254	0.254
Tajikistan	1	0.218	0.218
Cuba	1	0.179	0.179
Nigeria	1	0.177	0.177
Philippines	1	0.163	0.163
Mexico	1	0.095	0.095

section S3. Characterizing instances of reciprocity

When the directed daily average Goldstein time series of country A towards country B CCM causes country B's directed daily average Goldstein time series targeting country A (i.e. $CCM(A,B) \geq 0.25$ and $CCM(B,A) \geq 0.25$) we say that countries A and B are exhibiting "CCM reciprocity". Strictly speaking, this definition is necessary, but not sufficient, to show reciprocity between pairs of countries because CCM causation does not guarantee that influence respects valence. For example, although counter-intuitive, it is possible that country A's cooperative interactions with country B are causing B to act conflictingly towards A.

To demonstrate CCM reciprocity indicates direct reciprocity in the traditional sense, we compare the reactions between countries exhibiting CCM reciprocity to the reactions of pairs of countries without CCM reciprocity. While Fig. 2 of the main text examines conditional probabilities relative to global probabilities (i.e. the probability of cooperative, or conflictive (respectively),

interaction across the entire ICEWS dataset), Figure 25 compares the rate of cooperation (or conflict) given recent cooperation (or conflict) between pairs of countries relative to the aggregate probability of cooperation (or conflict) between that pair of countries. Pairs of countries exhibiting CCM reciprocity are more likely to cooperate given recent cooperation and more likely to conflict given recent conflict when compared to pairs of countries without CCM reciprocity.

We refine our characterization of CCM reciprocity by examining the response of country pairs to interactions of each Quad Class (see Section 2). Figures 26-29 demonstrate across different time windows after a particular interaction type (denoted Q) that country pairs with CCM reciprocity are more likely to engage in that interaction type in the subsequent day, three days, week, or month than country pairs without CCM reciprocity. Combined, the results in this section support the claim that CCM reciprocity is indeed indicative of direct reciprocity in the traditional sense because cooperative or conflictive interactions, or even specific Quad Classes of interactions, are reciprocated by country pairs with CCM reciprocity.

table S2. The Pearson correlation for proportion of interactions of each Quad Class between a pair of countries to the shared influence for that pair of countries.

Quad Class	Correlation (p-value)
Verbal Cooperation	0.184 (0.002)
Material Cooperation	-0.278 (0.003)
Verbal Conflict	-0.262 (0.005)
Material Conflict	-0.038 (0.685)

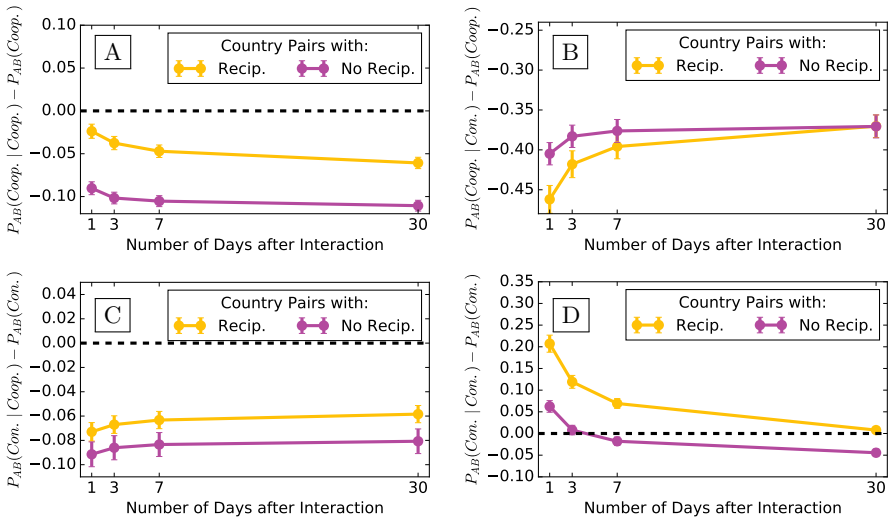

Figure 25: Country pairs exhibiting CCM reciprocity are more likely to reciprocate cooperation or conflict. Given an observation of cooperation (left) or conflict (right), reciprocating country-pairs (according to CCM analysis) are more likely to reciprocate (**(A)** & **(D)**) in the cumulative interactions in the following day, three days, week, and month (x-axis). Reciprocating country-pairs (according to CCM analysis) are less likely to deviate from their typical rates of cooperation given recent conflict, and they are less likely to deviate from their typical rates of conflict given recent cooperation (**(B)** & **(C)**). Each point represents the average rate of cooperation or conflict between countries A and B, denoted P_{AB}, for reciprocating country pairs (yellow) or non-reciprocating country pairs (purple) and error bars represent the standard error. Probabilities (y-axis) have been shifted according to the aggregate probabilities of cooperation or conflict, respectively, on a pair-by-pair basis (i.e. what is the probability that a randomly selected interaction between countries A and B across the entire ICEWS dataset is cooperation or conflict?).

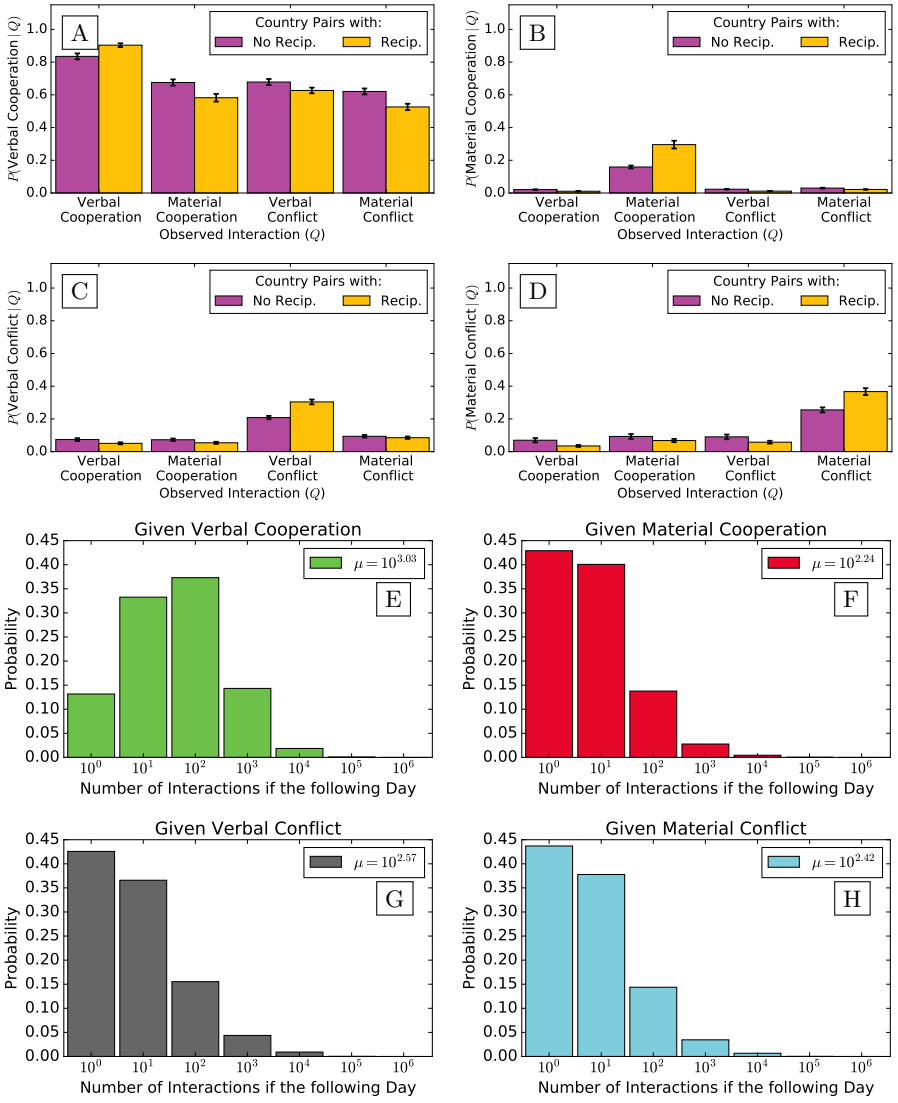

fig. S26. The patterns of behavior in the day following an interaction. Given an observed interaction type (x-axis, denoted Q) between a pair of countries with CCM reciprocity (yellow) or without (purple), we plot the cumulative probability (y-axis) of Verbal Cooperation **(A)**, Material Cooperation **(B)**, Verbal Conflict **(C)**, or Material Conflict **(D)** in the day following the interaction. We calculate the average rate of each Quad Class given each Quad class and represent the standard error of these distributions with error bars. **(E)**-**(H)** demonstrate the distribution of the number of interactions of any type in the day after an interaction of a particular Quad Class (title).

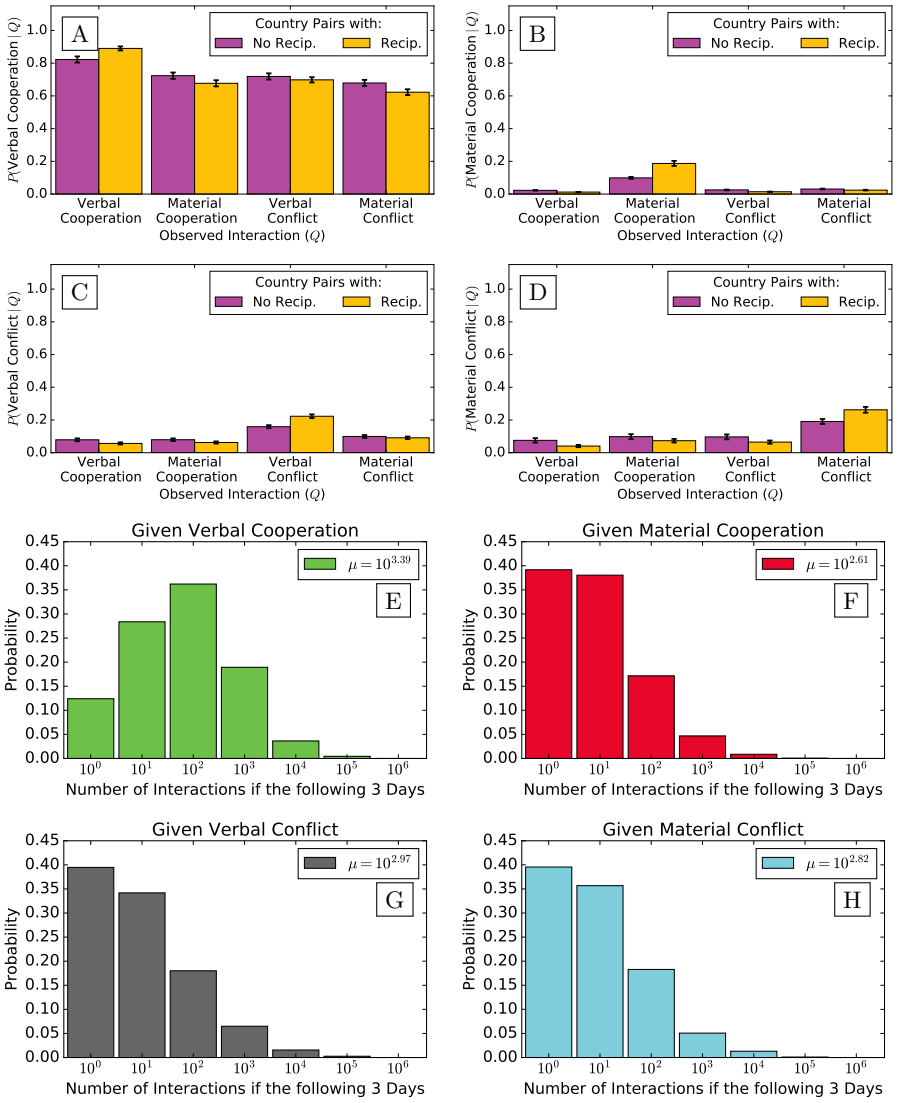

fig. S27. The patterns of behavior in the three days following an interaction. Given an observed interaction type (x-axis, denoted Q) between a pair of countries with CCM reciprocity (yellow) or without (purple), we plot the cumulative probability (y-axis) of Verbal Cooperation **(A)**, Material Cooperation **(B)**, Verbal Conflict **(C)**, or Material Conflict **(D)** in the three days following the interaction. We calculate the average rate of each Quad Class given each Quad class and represent the standard error of these distributions with error bars. **(E)**-**(H)** demonstrate the distribution of the number of interactions of any type in the three days after an interaction of a particular Quad Class (title).

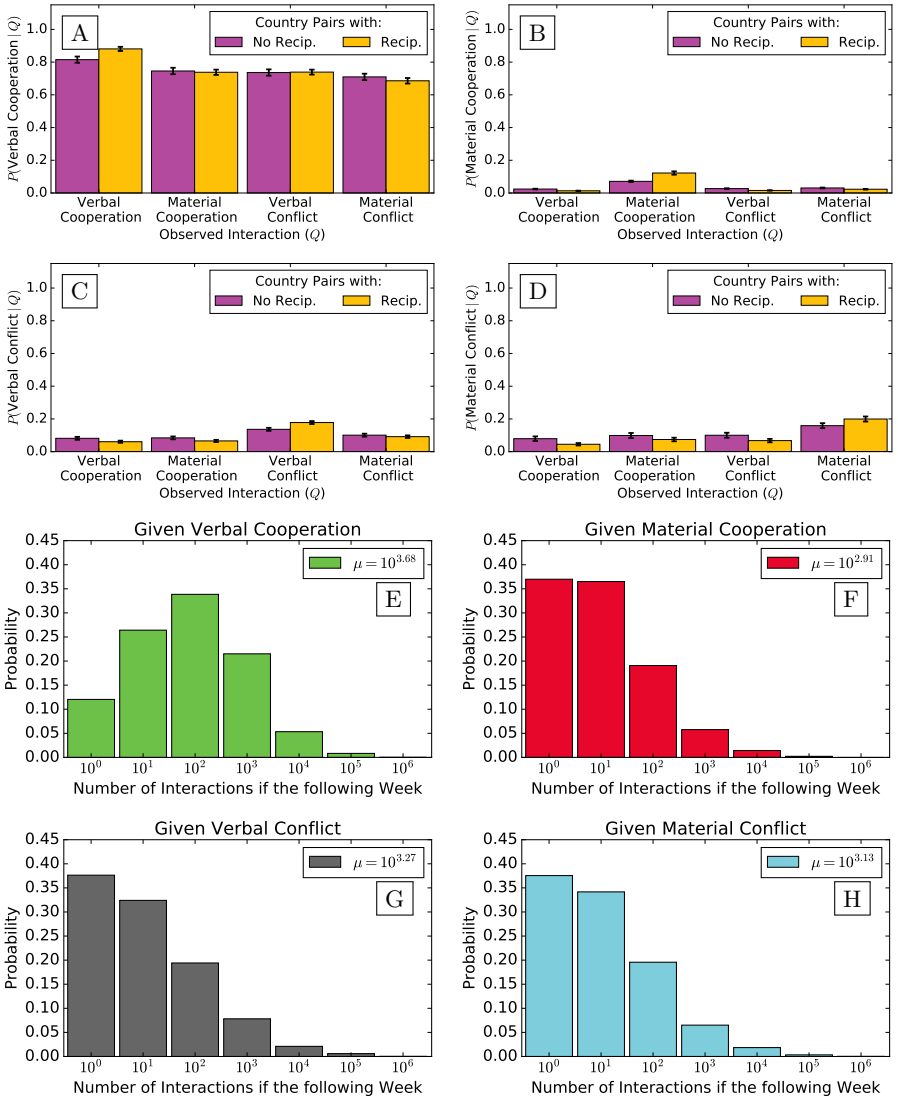

fig. S28. The patterns of behavior in the week following an interaction Given an observed interaction type (x-axis, denoted Q) between a pair of countries with CCM reciprocity (yellow) or without (purple), we plot the cumulative probability (y-axis) of Verbal Cooperation **(A)**, Material Cooperation **(B)**, Verbal Conflict **(C)**, or Material Conflict **(D)** in the week following the interaction. We calculate the average rate of each Quad Class given each Quad class and represent the standard error of these distributions with error bars. **(E)**-**(H)** demonstrate the distribution of the number of interactions of any type in the week after an interaction of a particular Quad Class (title).

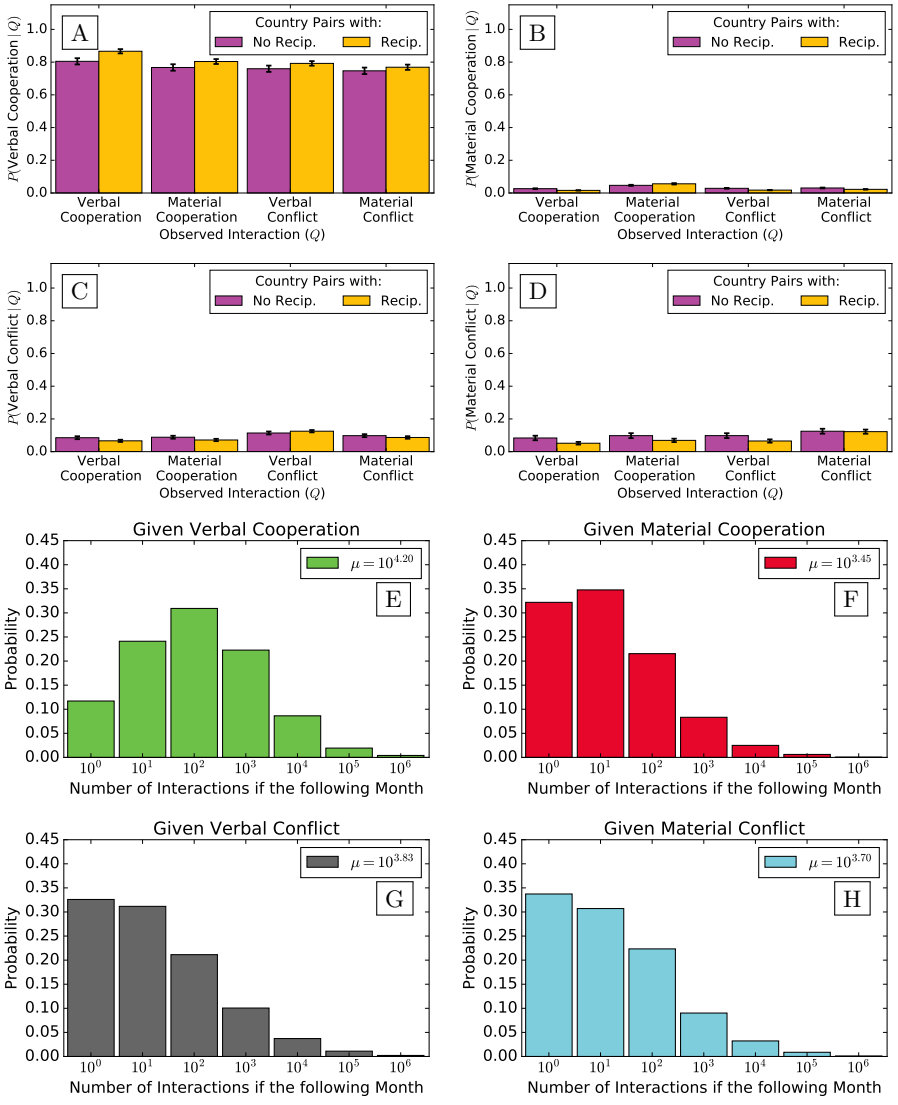

fig. S29. The patterns of behavior in the month following an interaction. Given an observed interaction type (x-axis, denoted Q) between a pair of countries with CCM reciprocity (yellow) or without (purple), we plot the cumulative probability (y-axis) of Verbal Cooperation **(A)**, Material Cooperation **(B)**, Verbal Conflict **(C)**, or Material Conflict **(D)** in the month following the interaction. We calculate the average rate of each Quad Class given each Quad class and represent the standard error of these distributions with error bars. **(E)**-**(H)** demonstrate the distribution of the number of interactions of any type in the month after an interaction of a particular Quad Class (title).

section S4. Varying thresholds for CCM reciprocity

According to CCM analysis (described in Section 2), countries A and B have reciprocity if $CCM(A,B) \geq 0.25$ and $CCM(B,A) \geq 0.25$ following the suggestion made by the creators of CCM in [33]. Here, we explore this threshold in context. In Figure 30A, we randomly shuffle the Goldstein time series of A's treatment of B and then apply CCM analysis to measure the influence of the permuted time series on B's empirical treatment of A as a null model. CCM values resulting from this null model are less than 0.1, which suggests that $CCM(A,B) \geq 0.25$ is a strict threshold for influence which is not obtained randomly. For un-shuffled time series, Figure 30B demonstrates the change in the number of country pairs with reciprocity as the minimum threshold for CCM influence is varied. To further explore the effects of perturbing the 0.25 threshold, we provide the map of reciprocity while varying the CCM threshold between 0.15 and 0.50 in Figures 31-38.

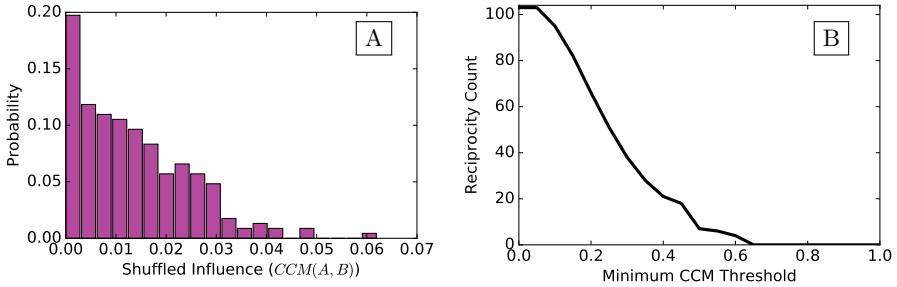

fig. S30. The effects of varying the CCM threshold for casuality. **(A)** Given the average daily Goldstein time series of country A's treatment of country B, and vice versa, we randomly permute the time stamps of and apply CCM analysis to test A's influence on B's treatment of A after permutation. **(B)** Changes in the number of country pairs with CCM reciprocity (y-axis) as the minimum CCM influence threshold (x-axis) is varied (using un-shuffled time series).

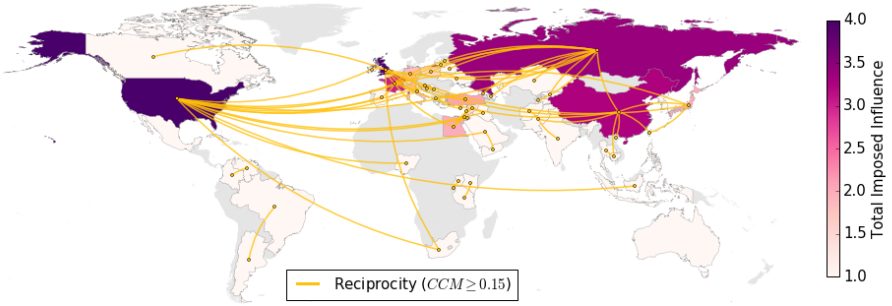

Figure 31: Pairs of countries exhibiting CCM reciprocity (i.e. $CCM(A, B) \geq 0.15$ and $CCM(B, A) \geq 0.15$) are connected using yellow edges. Countries are colored according to total imposed influence.

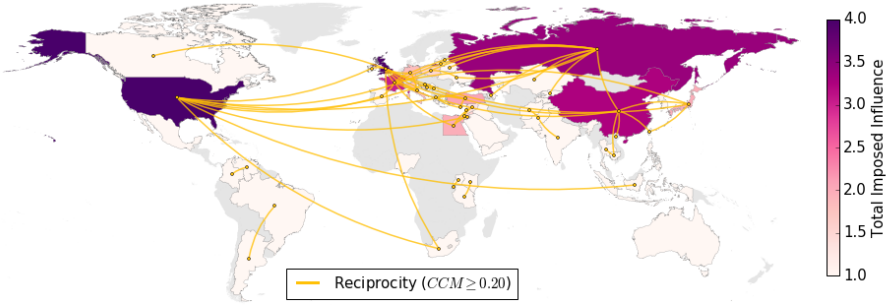

Figure 32: Pairs of countries exhibiting CCM reciprocity (i.e. $CCM(A, B) \geq 0.20$ and $CCM(B, A) \geq 0.20$) are connected using yellow edges. Countries are colored according to total imposed influence.

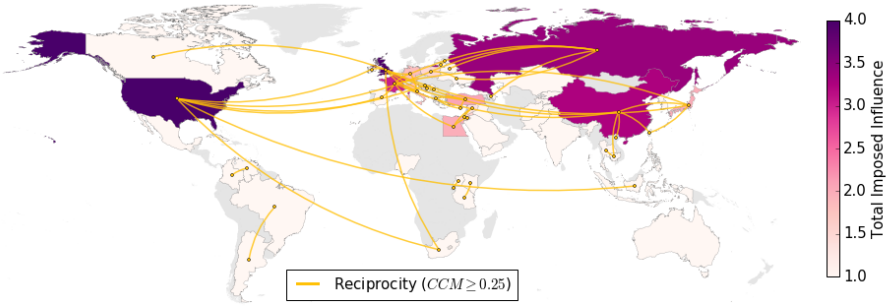

Figure 33: Pairs of countries exhibiting CCM reciprocity (i.e. $CCM(A, B) \geq 0.25$ and $CCM(B, A) \geq 0.25$) are connected using yellow edges. Countries are colored according to total imposed influence.

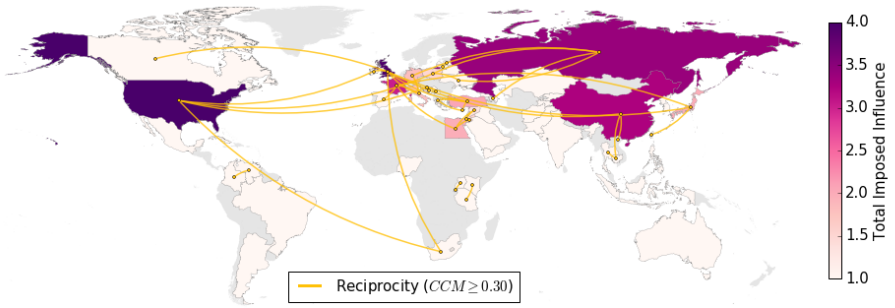

Figure 34: Pairs of countries exhibiting CCM reciprocity (i.e. $CCM(A, B) \geq 0.30$ and $CCM(B, A) \geq 0.30$) are connected using yellow edges. Countries are colored according to total imposed influence.

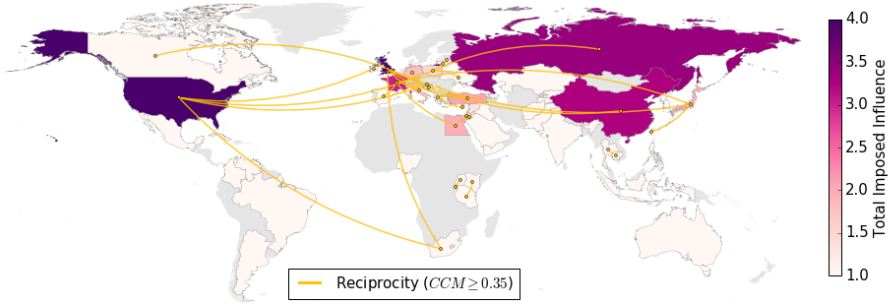

Figure 35: Pairs of countries exhibiting CCM reciprocity (i.e. $CCM(A, B) \geq 0.35$ and $CCM(B, A) \geq 0.35$) are connected using yellow edges. Countries are colored according to total imposed influence.

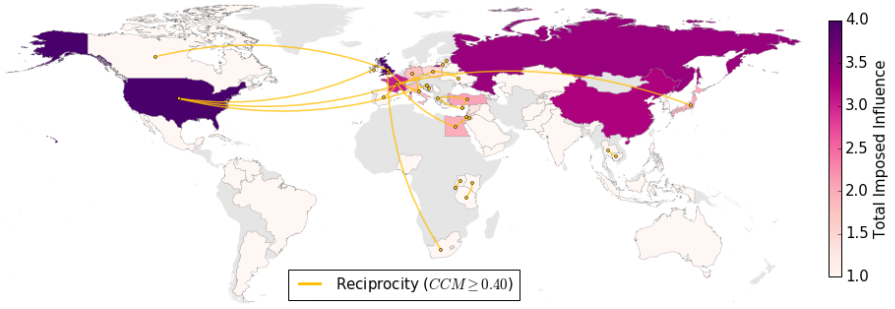

Figure 36: Pairs of countries exhibiting CCM reciprocity (i.e. $CCM(A, B) \geq 0.40$ and $CCM(B, A) \geq 0.40$) are connected using yellow edges. Countries are colored according to total imposed influence.

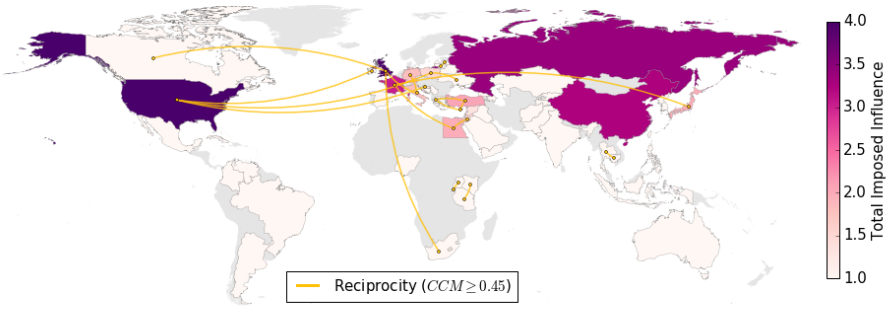

Figure 37: Pairs of countries exhibiting CCM reciprocity (i.e. $CCM(A, B) \geq 0.45$ and $CCM(B, A) \geq 0.45$) are connected using yellow edges. Countries are colored according to total imposed influence.

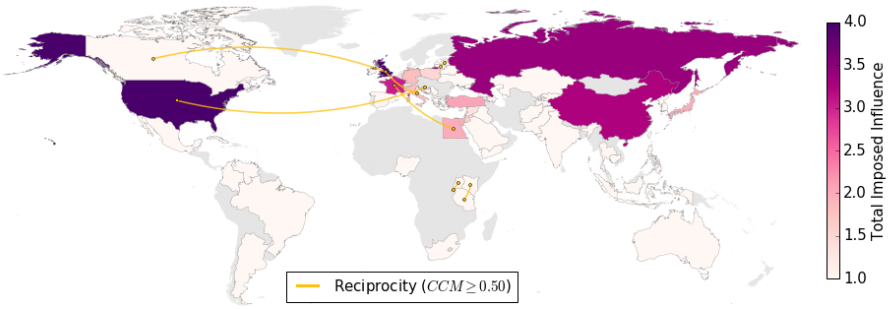

Figure 38: Pairs of countries exhibiting CCM reciprocity (i.e. $CCM(A, B) \geq 0.50$ and $CCM(B, A) \geq 0.50$) are connected using yellow edges. Countries are colored according to total imposed influence.

section S5. Country pairs with asymmetric influence

table S3. Country pairs ordered by increasing absolute difference in directed influence (i.e. $\mid CCM(A,B) - CCM(B,A) \mid$).

Country A	Country B	$CCM(A,B)$	$CCM(B,A)$	$\mid CCM(A,B) - CCM(B,A) \mid$
Russia	Ukraine	0.302	0.301	0.001
Russia	China	0.242	0.240	0.002
United Kingdom	Canada	0.547	0.545	0.002
South Korea	United States	0.106	0.103	0.003
Greece	Turkey	0.475	0.470	0.004
Georgia	Russia	0.181	0.176	0.005
United States	France	0.189	0.184	0.005
Japan	France	0.459	0.453	0.006
Pakistan	Afghanistan	0.228	0.222	0.007
Afghanistan	Iran	0.226	0.218	0.008
Germany	United Kingdom	0.300	0.291	0.009
Kazakhstan	Russia	0.254	0.244	0.009
Uganda	Rwanda	0.637	0.627	0.010
United States	Japan	0.086	0.075	0.011
France	Spain	0.444	0.430	0.014
Syria	Iran	0.237	0.221	0.016
South Korea	North Korea	0.278	0.262	0.016
Nigeria	United States	0.177	0.160	0.018
China	Taiwan	0.295	0.277	0.018
France	China	0.278	0.257	0.021
United States	Palestine	0.204	0.183	0.021
Cambodia	Thailand	0.476	0.453	0.023
Italy	United Kingdom	0.580	0.555	0.025
Lebanon	Israel	0.262	0.237	0.026
South Africa	United Kingdom	0.489	0.463	0.026
Cyprus	Turkey	0.491	0.464	0.027
Poland	United States	0.478	0.452	0.027
France	Germany	0.306	0.279	0.027
Tajikistan	Russia	0.218	0.187	0.031
United Kingdom	China	0.382	0.350	0.032
United States	Mexico	0.127	0.095	0.032
South Africa	United States	0.385	0.352	0.033
Italy	Germany	0.491	0.457	0.034
South Korea	China	0.232	0.197	0.035
United States	Syria	0.153	0.117	0.036
Israel	Egypt	0.199	0.163	0.036
Georgia	United States	0.177	0.140	0.037
Jordan	Israel	0.458	0.419	0.039
Russia	Belarus	0.322	0.282	0.040

Philippines	United States	0.163	0.120	0.042
Egypt	France	0.594	0.551	0.043
Bosnia and Herzegovina	Croatia	0.461	0.416	0.046
China	Vietnam	0.390	0.343	0.047
Russia	France	0.293	0.246	0.047
India	Pakistan	0.258	0.205	0.053
United Kingdom	Russia	0.222	0.166	0.055
Turkey	United States	0.203	0.146	0.057
Russia	Germany	0.360	0.301	0.059
Latvia	Lithuania	0.689	0.629	0.059
Italy	United States	0.248	0.188	0.060
China	Japan	0.317	0.254	0.063
Thailand	United States	0.148	0.085	0.063
North Korea	United States	0.331	0.268	0.064
United Kingdom	France	0.290	0.225	0.065
Iraq	Iran	0.161	0.095	0.067
Kyrgyzstan	Russia	0.299	0.231	0.068
Greece	Cyprus	0.555	0.487	0.069
United Kingdom	Turkey	0.462	0.393	0.069
Iran	Turkey	0.302	0.233	0.069
Ireland	United States	0.521	0.451	0.070
Poland	Ukraine	0.565	0.493	0.072
Australia	Indonesia	0.196	0.124	0.072
Azerbaijan	Russia	0.396	0.324	0.072
Colombia	Venezuela	0.388	0.312	0.075
United States	China	0.142	0.066	0.076
Ireland	United Kingdom	0.425	0.348	0.076
Croatia	Serbia	0.419	0.342	0.077
United States	Jordan	0.299	0.218	0.081
Israel	Palestine	0.274	0.193	0.081
Taiwan	Japan	0.474	0.390	0.084
China	Australia	0.200	0.115	0.085
Jordan	Egypt	0.551	0.464	0.087
China	Pakistan	0.243	0.156	0.087
Tanzania	Kenya	0.697	0.609	0.088
United States	Vietnam	0.236	0.147	0.089
Serbia	Bosnia and Herzegovina	0.339	0.247	0.092
Spain	United States	0.358	0.266	0.092
Syria	Lebanon	0.195	0.102	0.092
Cuba	United States	0.179	0.084	0.095
United States	Iran	0.212	0.116	0.096
South Korea	Japan	0.244	0.145	0.099

Egypt	Syria	0.428	0.329	0.100
Poland	Russia	0.456	0.355	0.100
United States	Croatia	0.705	0.605	0.100
China	Cambodia	0.411	0.307	0.105
United States	Russia	0.306	0.201	0.105
Brazil	Argentina	0.383	0.277	0.106
Iraq	United States	0.292	0.179	0.113
Indonesia	United States	0.369	0.250	0.119
Jordan	Palestine	0.321	0.191	0.131
Syria	Israel	0.454	0.320	0.134
Italy	France	0.499	0.364	0.135
North Korea	Japan	0.237	0.100	0.137
Turkey	Iraq	0.312	0.163	0.149
Japan	United Kingdom	0.556	0.397	0.159
Egypt	Palestine	0.240	0.075	0.165
Thailand	Myanmar	0.429	0.262	0.167
United States	Pakistan	0.253	0.079	0.173
Germany	Iran	0.384	0.208	0.176
United States	Ukraine	0.323	0.142	0.181
Taiwan	United States	0.161	-0.073	0.235
United States	Saudi Arabia	0.416	0.153	0.263
Yemen	Saudi Arabia	0.529	0.199	0.330

In Table 3, we only consider directed CCM influence scores where CCM analysis produced confident influence assessments (i.e. $p_{val} < 10^{-3}$). The country pairs with the largest influence asymmetry are comprised of wealthy and generally influential countries (see Section 2.4) paired with smaller countries with weaker economies. On aggregate, the difference in directed influence for a country pair is not related to the average cooperation-level describing their interactions (e.g. Pearson correlation for $GS(E_{A,B})$ and $\mid CCM(A,B) - CCM(B,A) \mid$ is $\rho = -0.10$, $p_{val} = 0.31$)